

## THERMODYNAMIC PROPERTIES FROM DIFFERENTIAL SCANNING CALORIMETRY BY CALORIMETRIC METHODS\*

JOSEPH H. FLYNN

*Institute for Materials Research, National Bureau of Standards, Washington, D.C. 20234 (U.S.A.)*

(Received 31 August 1973)

### ABSTRACT

Simple theory and techniques are explored and developed to utilize the differential scanning calorimeter for the determination of heat capacities, glass transition and enthalpies of transition between two thermodynamic states of substances. Effects due to the transition kinetics and thermal and electronic lags of the instrument are either corrected for or eliminated.

### INTRODUCTION

The calorimetric equations that relate enthalpy change to the area between traces from differential scanning calorimetry (DSC) were noted in the early literature<sup>1</sup>. However, since then, analytical techniques have focused upon the measurement of the amplitude of the power-difference coordinate, rather than the area bounded by the traces between two temperatures. Therefore, the treatment of data from DSC predominantly has made use of methods incorporating assumed thermokinetic mechanisms. This situation has been a carry-over from the necessary preoccupation of thermal analysis with the kinetics of heat flow in classical differential thermal analysis systems. Such methods are based on tenuous simplifying assumptions and gross approximations of rigorous but intractable heat flow equations.

However, Guttman and Flynn<sup>2</sup> have recently formalized methods based on fundamental thermodynamic considerations which should serve to redirect data analysis techniques away from these often irrelevant problems inherent in treatments based on kinetic mechanism. This methodology is further developed and extended in this paper.

### CALIBRATION OF ISOTHERMAL TEMPERATURE

The temperature calibration at any non-zero rate of temperature change involves corrections for lags within the system and for any difference between the

---

\*Presented at the 4th North American Thermal Analysis Society Meeting, Worcester, Mass., June 13-15, 1973.

programmed and sample temperatures. This calibration is discussed in a subsequent article. However, here we will show that the calibration of the programmed temperature of the DSC with the temperature of a sample within the sample cup may be effected for the isothermal case.

One assumption is made concerning the instrument at this point—baseline stability. That is, at any given temperature, there is a constant and reproducible net difference in power supplied to the two calorimeters to overcome their respective heat leaks.

The effect of a change of the programmed temperature upon the net power difference ( $\delta\dot{q}$ ) between the two covered calorimeter cups, each containing empty sample containers and lids, is shown in Fig. 1a. The programmed temperature is raised 0.1 K increments from 427.8 to 428.5 K. A transient deflection of the baseline occurs at each increment. (The manner in which the temperature change is accomplished is not relevant, e.g., either by changing the temperature at constant rate or, as in Fig. 1, by an instantaneous turn of the temperature programming knob.)

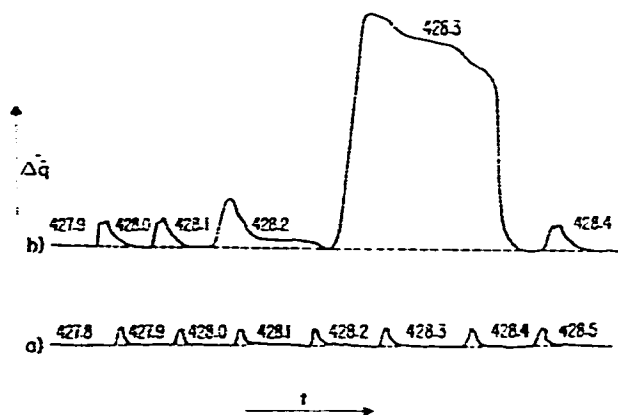


Fig. 1. DSC trace (differential power vs. time) of successive isothermals for empty calorimeters and for fusion of indium. Chart speed 1 in./min; Range 2. a) empty sample containers; b) 8.0 mg of 99.99 indium in sample calorimeter. Numbers represent programmed temperatures. Temperature change occurs at the beginning of each deflection.

The difference in heat leaks of the sample and reference calorimeters is assumed linear with temperature over the short temperature intervals in Fig. 1a. Therefore, a straight baseline is constructed connecting the isothermals. The area between the deflection and the baseline,  $A_2(T_2, T_1)$ , for the temperature change,  $T_1 \rightarrow T_2$ , for trace a is

$$A_2(T_2, T_1) = \int [\delta(t) - \delta_0(t)] dt = \kappa^{-1} \int_{T_1}^{T_2} (C_S - C_R) dT \quad (1)$$

where  $\kappa$  is an enthalpic rate calibration factor,  $[\delta(t)$  and  $\delta_0(t)]$  is the deflection of trace a from the baseline at time,  $t$ , and  $C_S$  and  $C_R$  are the heat capacities of the

sample and reference calorimeters, respectively. Here, in eqn (1), and in the equations to follow, a measured amount of heat supplied to a material, determined by an experimental area, is identified with the enthalpy difference of the material at two temperatures. It assumes implicitly that the experimental time scale is such that initial and final measurements are made at times sufficient for the materials reasonably to approach stable or metastable thermodynamic states. This problem becomes much more critical during the rapid temperature changes inherent in methods of dynamic enthalpic analysis, in which, at best, "steady" rather than stationary states are approached.

The effect of an 8.0 mg sample of indium, sealed in the sample container within the sample calorimeter, upon the trace of an experiment similar to that shown in Fig. 1a is shown in Fig. 1b. Here, the area between the deflection and the isothermal baseline for a temperature change,  $T_1 \rightarrow T_2$ , is

$$A_b(T_2, T_1) = \kappa^{-1} \left\{ \int_{T_1}^{T_2} (C_s - C_R) dT + \int_{T_1}^{T_2} C_s dT + h_s(T_2, T_1) \right\} \quad (2)$$

where  $C_s$  is the heat capacity of the sample and  $h_s(T_2, T_1)$  is any heat of transition occurring in the sample during the temperature change,  $T_1 \rightarrow T_2$ .

The large deflection from the baseline in Fig. 1b between 428.1 and 428.2 K is due to premelting phenomena, and the exceptionally large deflection for the temperature change, 428.2–428.3 K, identifies this programmed temperature interval with the melting point of indium.

In this fashion, the programmed temperature may be calibrated under isothermal conditions with a degree of accuracy dependent upon the sensitivity of the temperature programmer and the accessibility of a sufficient range of calibrating substances with sharp, well-characterized transition temperatures. (On some instruments, temperature intervals must be larger than those in Fig. 1, so that short-lived electronic effects do not bias the area calculations.)

If it is assumed that the sample, sealed in an aluminum container within the covered calorimeter cup, has no effect on the heat leak, or any such effect is independent of temperature over the range,  $T_1 \rightarrow T_2$ , eqn (1) may be subtracted from eqn (2) to obtain

$$A_b(T_2, T_1) - A_a(T_2, T_1) = \kappa^{-1} \left\{ \int_{T_1}^{T_2} C_s dT + h_s(T_2, T_1) \right\} \quad (3)$$

which relates the thermodynamic properties of the sample,  $C_s$  and  $h_s$ , to experimental areas. Thus, if  $C_s$  and  $h_s$  are known over the interval,  $T_1 \rightarrow T_2$ , the calibration factor,  $\kappa$ , may be calculated. Conversely if  $\kappa$  is known,  $C_s$  may be calculated for temperature intervals for which  $h_s = 0$  from the area differences in eqn (3). If the value of  $C_s$  has been determined, this relatively small heat capacity integral may be subtracted from eqn (3) and the enthalpy of transition calculated.

The experimental method in this section may be used in conjunction with the Van't Hoff equation to determine the purity of ideal solutions<sup>3</sup>.

## DETERMINATION OF HEAT CAPACITY

A calculation of heat capacity from the experiment in Fig. 1 of the previous section would involve differences in small areas over short temperature intervals. The experimental accuracy may be increased by utilizing a larger temperature interval. The results of such an experiment are shown in Fig. 2.

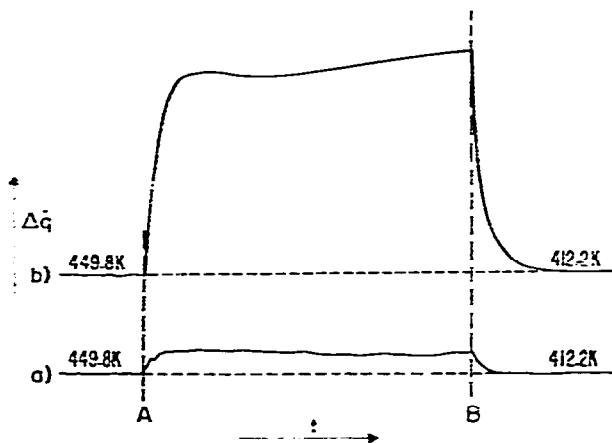


Fig. 2. DSC trace for empty calorimeters and for heat capacity of  $\alpha\text{-Al}_2\text{O}_3$  at constant programmed temperature change. Chart speed 1 in./min; Range 8;  $\dot{T}_p = -10$  K/min. a) empty sample containers; b) 130 mg of  $\alpha\text{-Al}_2\text{O}_3$  in sample container. Numbers represent calibrated isothermal temperatures. Programmed temperature change began at time, A; stopped at B.

The empty containers (curve 2a), which were maintained at a calibrated isothermal temperature of 449.8 K, are cooled at a programmed rate of 10 K/min (the corrected cooling rate varies between 9.5 and 9.1 K/min due to the change in slope of the temperature calibration curve in this region). The cooling is discontinued and the system is maintained at a calibrated isothermal temperature of 412.2 K.

An experiment differing only in that a 130 mg disc of  $\alpha\text{-Al}_2\text{O}_3$  is sealed in the sample container is shown by curve 2b.

An average value for the heat capacity,  $\overline{C}_s(T_2, T_1)$  may be obtained from the difference of the two areas between curves 2b and 2a and their respective isothermal baselines, as the integration of eqn (3) between  $T_1$  and  $T_2$ , assuming  $h_s(T_2, T_1) = 0$ , yields

$$\overline{C}_s(T_2, T_1) = \frac{\kappa[A_b(T_2, T_1) - A_a(T_2, T_1)]}{T_2 - T_1} \quad (3')$$

As is the case in the previous section, the areas do not depend upon the mode by which the temperature change was accomplished.

An average heat capacity is determined in all methods of calorimetric measurement involving isothermal interruption. Narrowing the span of the temperature

interval in any individual experiment involves accommodation to the requirements for precision in the measurement of area and temperature differences.

The linear extrapolation of the baselines in the calculation of the areas in eqn (3') over a single large jump may introduce an error if the curvature of the baseline is altered by the presence of a sample. Any such baseline curvature may be followed better by summing the areas of a series of short temperature jumps over the interval  $T_1 \rightarrow T_2$ . Such a summation cancels out any inaccuracies in the measurement of the intermediate individual temperature intervals.

In this use of the DSC as a calorimeter, a metered temperature change is produced in the system, and the compensating amount of power is measured. This may be contrasted with traditional calorimetry in which a metered amount of power is added to the system and the compensating temperature change measured.

Both cases determine a mean heat capacity over a temperature interval. Instantaneous heat capacities are obtained only in scanning methods. However, here the thermal lag in many materials, especially organic polymers, complicates definition of the instantaneous thermodynamic state of the material.

An accurate value for the change in enthalpy of  $\alpha\text{-Al}_2\text{O}_3$  over the temperature interval in Fig. 2 is available in the literature<sup>4</sup>. This value and the difference in areas between curves 2a and 2b and their respective isothermal baselines result in a value for the calibration factor,  $\kappa$ . This value is four percent lower than a  $\kappa$  calculated from the area under the heat of fusion curve of 8.0 mg of 99.99% indium at 429 K on the same instrument.

#### DETERMINATION OF GLASS TRANSITION TEMPERATURE

The glass transition temperature is usually defined as that temperature at which there exists a discontinuity in the slope of the temperature-enthalpy curve, e.g., the temperature of intersection of the enthalpy curves of the supercooled liquid and glassy states of a substance. Unfortunately, the application of this simple definition to thermal analysis data is often beclouded by complicating factors.

Some of these factors may be illustrated in the schematic enthalpy-temperature plot in Fig. 3. The solid line, 2, represents the supercooled liquid state of the system. Rapid cooling from  $T_2$  (dotted line a) results in the formation of a metastable glassy state represented by line 1'. Slow cooling from  $T_2$  (dotted line b) results in the formation of a different metastable state represented by line 1.

The intersection of the extrapolated enthalpy curves for states 1 and 2 defines the glass transition temperature,  $T_{G,1}$ , between states 1 and 2 at which  $H(\text{state 1}) = H(\text{state 2})$  and the slope of the enthalpy curve changes discontinuously from  $C_1$  to  $C_2$ . The intersection of the extrapolated enthalpy curves for states 1' and 2 similarly defines the glass transition temperature,  $T_{G,1'}$ , between states 1' and 2.

A glass transition temperature might be determined from an experiment similar to that illustrated in Fig. 1 by noting the temperature interval in which the heat capacity changed abruptly. If the temperature intervals were small, the deter-

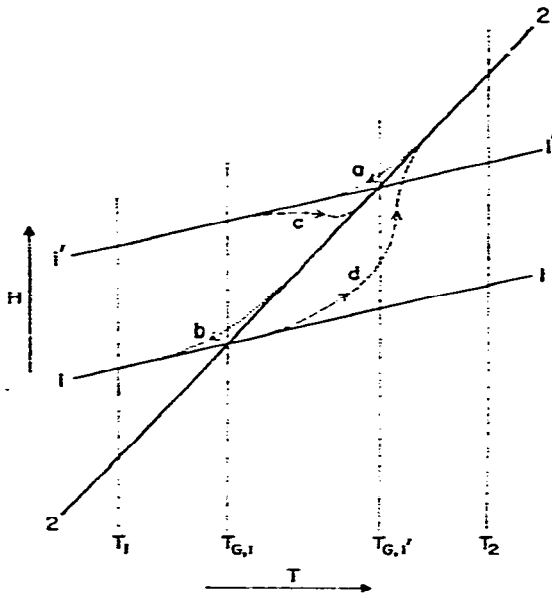


Fig. 3. Enthalpy-temperature schematic in glass transition region. Supercooled liquid, line 2; metastable glass, line 1; metastable glass, line 1'.  $T_{G,1}$ , glass transition temperature between states 1 and 2;  $T_{G,1'}$ , glass transition temperature between states 1' and 2;  $T_1$ ,  $T_2$ , temperatures outside of region of glass transition kinetics. Curve a: state 2  $\rightarrow$  state 1' (rapid cooling); Curve b: state 2  $\rightarrow$  state 1 (slow cooling); Curve c: state 1'  $\rightarrow$  state 2 (slow heating); Curve d: state 1  $\rightarrow$  state 2 (rapid heating).

mination of heat capacities from the area differences would require an apparatus of very great sensitivity and an extremely accurate measurement of the temperature interval. In any event, such a measurement involves the kinetics of the transition in its determination.

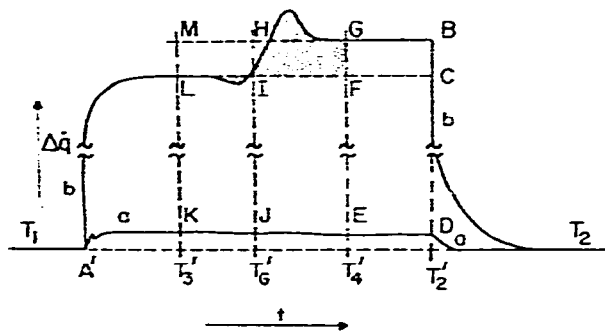


Fig. 4. Idealized DSC trace for a glass transition. a) empty sample containers; b) sample with glass transition at  $T_G$  in sample container,  $T_1$ ,  $T_2$ , calibrated isothermal temperatures;  $T_3$ ,  $T_G$ ,  $T_4$ ,  $T_2$ , calibrated temperatures at heating rate,  $\dot{T}_p$ . System isothermal at  $T_1$  until time, A; heated at rate,  $\dot{T}_p$ , until time, BD; isothermal at  $T_2$  after BD.

If, to avoid kinetic complications, the temperature jump interval is increased to extend from a temperature,  $T_1$ , well below the glass transition temperature,  $T_G$ , to a

temperature,  $T_2$ , above  $T_G$ , as shown in Fig. 4, then eqn (3) becomes

$$\kappa[A_b(T_2, T_1) - A_a(T_2, T_1)] = \int_{T_1}^{T_G} C_1 dT + \int_{T_G}^{T_2} C_2 dT \quad (3'')$$

where  $C_1$  and  $C_2$  are the heat capacities for the thermodynamic states below and above the glass transition, respectively. It is assumed that no first order transition occurs in the range  $T_1 \rightarrow T_2$ , (i.e.,  $h_s = 0$ ). Equation 3'' is a mathematical description of  $T_G$  as the point of discontinuity in the slope of the enthalpy curve and  $T_G$  may be experimentally determined if the heat capacities,  $C_1$  and  $C_2$ , are known.

If  $C_1$  and  $C_2$  are assumed to be independent of temperature over the range,  $T_1 \rightarrow T_2$  (see Fig. 4), then

$$T_G = \frac{T_2 C_2 - T_1 C_1 - \kappa[A_b(T_2, T_1) - A_a(T_2, T_1)]}{C_2 - C_1} \quad (4)$$

Unfortunately, the use of eqn (4) to determine  $T_G$  requires extremely accurate values for  $C_1$ ,  $C_2$  and the large area between the traces b and a in Fig. 4.

However, Guttman<sup>5</sup> has suggested a method to obtain the glass transition temperature, which, although it utilizes the DSC in the scanning mode, is based on thermodynamic concepts and may be divorced, to a large extent, from kinetic processes. Since this method involves only the area sensitive to the glass transition (the shaded area between LG and LIF in Fig. 4), it avoids the problem with eqn (4) of determining small differences between large numbers.

The assumption is made that during a scan at a programmed heating rate,  $\dot{T}_p$ , a temperature,  $T'_3$ , may be chosen in a temperature range in which the DSC trace is representative of the initial thermodynamic state, i.e., that it is removed both from initial transients and thermokinetic effects associated with the transition. Also, that a second temperature,  $T'_4$ , may be chosen, following the transition, similarly representative of the final thermodynamic state beyond the transition. The sample temperatures,  $T'_3$ ,  $T'_G$  and  $T'_4$  are calibrated at the programmed scan rate,  $\dot{T}_p$ . Temperature calibration for the scanning modes is discussed elsewhere<sup>6</sup>.

The total enthalpy change between  $T'_3$  and  $T'_4$  in Fig. 4 will be proportional to the area between trace b and trace a, i.e.,

$$\kappa(\text{AREA KLGE}) = H_{1,T'_G} - H_{1,T'_3} + H_{2,T'_4} - H_{2,T'_G} \quad (5)$$

where  $H_{1,T'}$  is the enthalpy of state 1 at temperature,  $T'$ , and  $H_{2,T'}$  is the enthalpy of state 2 at  $T'$ . This equation is an integrated form of eqn (3'') and defines  $T'_G$  as the temperature of intersection of the enthalpy curves of states 1 and 2,  $H_{1,T'_G} = H_{2,T'_G}$  being previously assumed.

If the traces before and after the transition are constant with temperature, then the heat capacities of the two states,  $C_1$  and  $C_2$  are independent of temperature, and

$$\begin{aligned} H_{1,T'} - H_{1,T'_3} &= C_1(T' - T'_3) \\ H_{2,T'} - H_{2,T'_3} &= C_2(T' - T'_3) \end{aligned} \quad (6)$$

The extrapolation of state 1 through  $\overline{\text{LIF}}$  in Fig. 4 gives

$$\kappa(\text{AREA } \overline{\text{KLFE}}) = H_{1,T'_4} - H_{1,T'_3} \quad (7)$$

The residual area obtained from the subtraction of eqn (7) from eqn (5) is

$$\begin{aligned} \kappa(\text{AREA } \overline{\text{LGF}}) &= \kappa(\text{AREA } \overline{\text{KLGE}}) - \kappa(\text{AREA } \overline{\text{KLFE}}) \\ &= (H_{2,T'_4} - H_{2,T'_G}) - (H_{1,T'_4} - H_{1,T'_G}) \\ &= C_2(T'_4 - T'_G) - C_1(T'_4 - T'_G) \end{aligned} \quad (8)$$

and the glass transition temperature,  $T'_G$  is

$$T'_G = T'_4 - \frac{\kappa(\text{AREA } \overline{\text{LGF}})}{C_2 - C_1} \quad (9)$$

The distance,  $\text{GF} = \text{HI} = \text{ML}$ , is equal to  $\hat{T}(\rho\kappa)^{-1}(C_2 - C_1)$ , so we obtain for  $T'_G$ ,

$$T'_G = T'_4 - \frac{\text{AREA } \overline{\text{LGF}}}{\text{GF}} \cdot \hat{T}\rho^{-1} \quad (4')$$

where  $\hat{T}$  is the heating rate (K/min) and  $\rho$  is the chart speed (unit length/min). Thus the glass transition temperature,  $T'_G$ , defined as the point of intersection of the enthalpies of the initial and final states, is determined in eqn (4') from the ratio of the enthalpy difference to the heat capacity difference between the two states, as the large enthalpies common to both states in Fig. 4 and eqn (4) have been eliminated and the area of interest,  $\text{AREA } \overline{\text{LGF}}$ , now includes only the shaded area minus the hatched area in Fig. 4.

The complications due to the kinetics of the transition have been avoided by the extrapolations from  $T'_3$  and  $T'_4$ . However, it is impossible, with a programmed temperature change, to escape effects due to electronic lags within the instrument and thermal lags within the calorimeter, the sample, and the interface between them<sup>6</sup>.

The calculation of the magnitude of the correction to eqn (4') to take into account these lags depends upon the mathematical model used to describe them and their coupling with one another and upon the temperature calibration procedure. For samples with low thermal conductivities, such as organic polymers, these lags may amount to several degrees at typical scan rates of 2–20 degrees per minute<sup>6</sup>.

Because of the uncertainties involved in the application of these corrections (particularly in the thermal lag in the sample), it is prudent to determine  $T'_G$  from eqn (4') for a series of scans at different rates of heating and extrapolate any variation in  $T'_G$  to zero heating rate. All samples in such a series of experiments must be initially at the same enthalpy state, i.e., previously cooled from the liquid state at the same rate of temperature change.

If the heat capacities,  $C_1$  and  $C_2$ , change linearly with temperature at different rates, the traces before and after the transition again will be linear but will differ in slope as illustrated in Fig. 5.



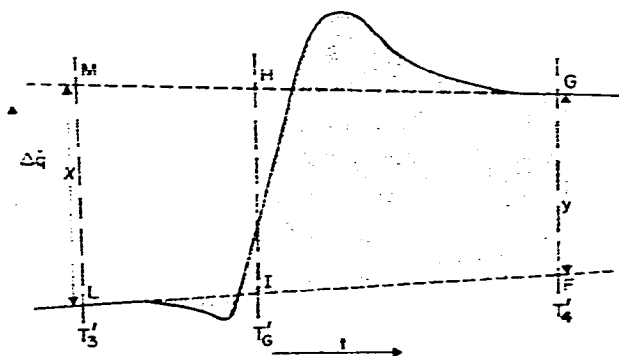


Fig. 5. DSC trace for a glass transition in which heat capacities are temperature dependent.  $T'_3$ ,  $T'_G$  and  $T'_4$  and letters are as in Fig. 4.  $x$  = distance  $ML$ ;  $y$  = distance  $GF$ .

A development similar to that used to obtain eqn (4') produces a quadratic in  $T'_G$ . If, in Fig. 5

$$x = \overline{ML} = (\rho\kappa)^{-1} \hat{T} (C_{2,T'_3} - C_{1,T'_3})$$

and

$$y = \overline{GF} = (\rho\kappa)^{-1} \hat{T} (C_{2,T'_4} - C_{1,T'_4})$$

the  $T'_G$  may be calculated from either

$$T'_G = \frac{T'_3 y - T'_4 x}{y - x} + \frac{(T'_4 - T'_3)}{y - x} \sqrt{y^2 + \frac{2 \hat{T} (x - y) \text{AREA } \overline{LGF}}{\rho (T'_4 - T'_3)}} \quad (4'')$$

or, equivalently,

$$T'_G = T'_4 - \frac{y(T'_4 - T'_3)}{y - x} \left\{ 1 - \sqrt{1 - \frac{2 \hat{T} (y - x) \text{AREA } \overline{LGF}}{y^2 \rho (T'_4 - T'_3)}} \right\}$$

$$(x \neq y)$$

$T'_G$  may be imaginary for  $y > x$ , resulting from a complicating endothermic reaction in the same region.

It is possible for a small exotherm to occur below  $T'_G$  if the rate at which the sample was previously quenched was more rapid than the rate at which it is heated as is the case for curves a and c in Fig. 3. This is indicated by the hatched areas in Figs. 4 and 5. This enthalpic drift below  $T'_G$  is kinetically sluggish and may be unresolvable at the sensitivity of most scanning instruments.

The measurement of these drifts by high precision adiabatic calorimetry has been reviewed by Chang<sup>7</sup>.

If the rate at which the sample is heated is greater than the rate at which it was previously quenched as is the case for curves b and d in Fig. 3, then an endothermic

peak will occur immediately after the glass transition. This peak often is present in DSC traces and may be quite large at a rapid heating rate. It is included in the shaded regions in Figs. 4 and 5 used to calculate the area  $\overline{LGF}$ . The traces in Figs. 4 and 5 are schematic. The exo- and endothermic drifts never both occur in a single scan.

Two DSC traces for a sample of polyvinyl chloride heated through its glass transition are shown in Fig. 6. In curve a, the sample had been cooled at a rate of 20 K/min while, in curve b, it had been cooled at 0.625 K/min. The heating rate for both scans was 20 K/min.

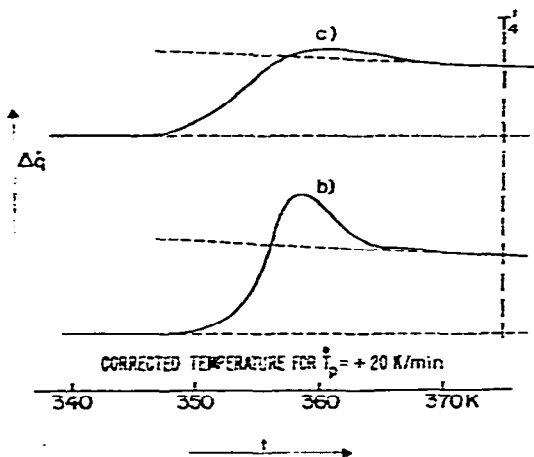


Fig. 6. DSC traces for glass transition of polyvinyl chloride. Chart speed: 4 in./min; Range 4;  $\dot{T}_p = 20$  K/min; weight = 27.9 mg. a) Cooled from 390 K to 200 K at  $\dot{T}_p = -20$  K/min; b) Cooled from 390 K to 200 K at  $\dot{T}_p = -0.625$  K/min.

If the midpoints between the initial and final heat capacity curves were used to define the glass transition temperature, then the more rapidly cooled sample in scan a would have a lower value (353.0 K) than the slowly cooled sample in scan b (354.5 K).

However, treatment of the scans with Guttman's method (eqn (4')) reverses the rank of the glass transition temperatures—352.2 K for the rapidly annealed scan and 351.8 K for the slowly annealed scan. This latter rank is in agreement with predictions from the thermodynamic model in Fig. 3.

#### DETERMINATION OF HEAT OF TRANSITION

The heat of transition can be measured by the method already described in this paper (Fig. 1), in which the temperature was increased over successive small increments. Thus, the heat of fusion of indium may be calculated from eqn (2) by summing the  $h_s(T_2, T_1)$  terms for the temperature increments. The heat capacity integrals for the calorimeter cups and the sample may be calculated from the areas of temperature increments for which  $h_s(T_2, T_1) = 0$ . These heat capacity terms should be no more than several percent of  $h_s$  for short temperature intervals.

The heat of a transition taking place over a broad temperature range, such as is the case for the fusion of polymers, could be measured by a large and rapid temperature jump from well below to above the transition temperature. This avoids the problem of the perception of the gradual departure and return to the baseline before and after the transition. Also, any complicating effects of side reactions, such as recrystallization, which may occur during a slow scan through the transition region, would be eliminated by this "drop" calorimetric method. The great disadvantage here is that large heat capacity integrals must be subtracted from the area to obtain the heat of transition.

The DSC trace at constant programmed temperature change often will follow a single straight line function before and after a transition. In this case the heat of transition may be calculated from the area between the trace and the constant baseline extrapolated from before and after the transition, and the heat capacity integrals in eqn (2) need not be determined.

However, if the sensitivity of the instrument is sufficient to detect a shift in the trace before and after the transition, the manner of drawing the baseline becomes important. Large shifts in baseline do occur in cases in which the heat capacities of the initial and final states differ appreciably. This obviously is the case where a change in the mass of the sample takes place, e.g., vaporization.

Various procedures have been proposed in the past for drawing the baseline which either were based on assumed thermokinetic mechanisms or arbitrarily posited its construction. However Guttman and Flynn<sup>2</sup> have recently devised a method of computing the enthalpy of transition independent of kinetic effects. The derivation is similar to that used in the development of eqn (4') for  $T'_G$ .

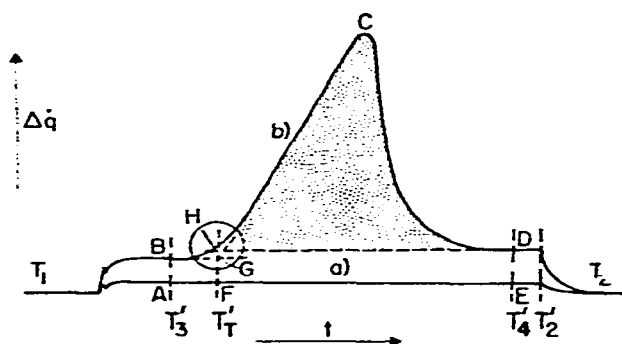


Fig. 7. Idealized DSC trace for a first-order transition. a) empty sample container; b) sample with first order transition in sample container.  $T_1$ ,  $T_2$ , calibrated isothermal temperature;  $T_3$ ,  $T'_$ ,  $T_4$ ,  $T'_$ , calibrated temperatures at heating rate,  $T'_$ . Temperature programmed as in Fig. 4.

An idealized trace for a first order transition is illustrated in Fig. 7. The example and discussion are for an endothermic reaction scanned at a constant heating rate. These may be applied, mutatis mutandis, to exothermic reactions and at constant cooling rate. The interpretation of Fig. 7 is identical to that of Fig. 4.  $T_1$  and  $T_2$  are

initial and final isothermal temperatures and the temperature is increased at a constant programmed rate,  $\dot{T}_p$ , between them.  $T'_3$  and  $T'_4$  lie, respectively, before and after kinetic effects associated with the transition.

The equation for the difference in area between traces b and a will take the form

$$\kappa[A_b(T_2, T_1) - A_a(T_2, T_1)] = \int_{T_1}^{T_T} C_1 dT + \int_{T_T}^{T_2} C_2 dT + h_T \quad (3''')$$

where  $T_T$  is the transition temperature and  $h_T$  is the heat of transition at temperature  $T_T$ .

In eqn (3''), the area under a second order transition uniquely defined  $T_G$ . However, in the case of a first order transition, two experimental parameters must be determined,  $T_T$  and  $h_T$ . The solution to this problem used by Guttman and Flynn<sup>2</sup>, and generally used by thermodynamicists, is to assign a value to the transition temperature based on experimental observation and determine  $h_T$  at this somewhat subjectively chosen temperature, consoled by the knowledge that if the enthalpy of transition is desired at any other temperature, it may be calculated from Kirchhoff's equation.

There is considerable evidence that, for a DSC trace, the experimental parameter most closely related to the transition temperature of a sharp, first order transition is the extrapolated onset temperature, calibrated at the scan rate of interest. This is represented by  $T'_T$  in Fig. 7 and is used in this section as the temperature at which the enthalpy of transition is determined.

The same assumptions as in the  $T_G$  determination are made, viz.: 1) baseline stability, 2)  $T'_3$  and  $T'_4$  may be chosen at points where the trace is representative of thermodynamic states respectively before and after the transition, and 3) extrapolation of the heat capacity is permissible from  $T'_3$  to  $T'_T$  and  $T'_4$  to  $T'_T$ .

The same development used to determine  $T_G$  (eqns (5), (6), (7) and (8)) permits the following identifications to be made between areas in Fig. 7 and thermodynamic properties in eqn (3'')<sup>2</sup>.

$$\kappa(\text{AREA } \overline{\text{ABCDE}}) = \int_{T'_3}^{T'_T} C_1 dT + \int_{T'_T}^{T'_4} C_2 dT + h_T$$

$$\kappa(\text{AREA } \overline{\text{ABGF}}) = \int_{T'_3}^{T'_T} C_1 dT$$

$$\kappa(\text{AREA } \overline{\text{FHDE}}) = \int_{T'_T}^{T'_4} C_2 dT$$

Thus the heat of transition,  $h_T$ , can be determined from the shaded area in Fig. 7, since

$$\begin{aligned} \kappa(\text{AREA } \overline{\text{BCDHG}}) &= \kappa(\text{AREA } \overline{\text{ABCDE}}) - \kappa(\text{AREA } \overline{\text{ABGF}}) - \kappa(\text{AREA } \overline{\text{FHDE}}) \\ &= h_T. \end{aligned} \quad (10)$$

Examples of the application of this method to specific cases, especially in the region encircled in Fig. 7 are shown in Fig. 8. The shaded areas are to be added and the hatched areas to be subtracted from the total area used to determine  $h_T$  from eqn (10).

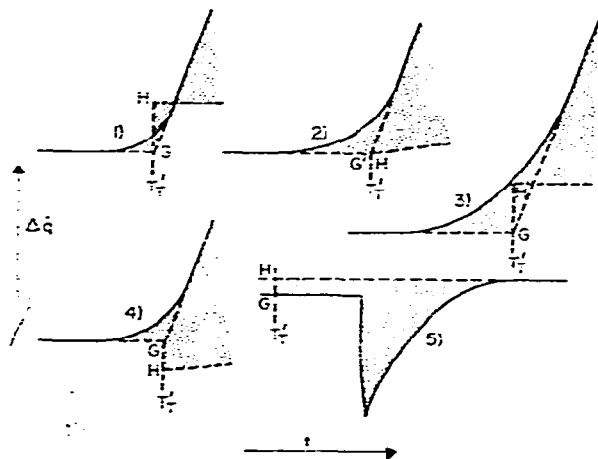


Fig. 8. Details of area calculation of the region of the onset temperature.  $T_T$ ,  $G$  and  $H$  as in Fig. 7. 5) represents exothermic solidification of a supercooled liquid ( $T_p < 0$ ).

There is again temperature correction due to the heat capacity change which is similar to that of the glass transition case. However, here it is a small correction term to what is in itself a small heat capacity correction to the enthalpy. Therefore, usually it may be neglected.

A prevalent method for the determination of areas under thermal analysis traces with baseline shifts is the construction of a straight line connecting the points of departure and return of the trace to the respective baselines that preceded and followed the transition<sup>8</sup>. That method is thermodynamically equivalent to defining the heat of transformation over a temperature interval during which the difference in the heat capacities between the two states changes in a linear manner with respect to time (zero order kinetics). Not only does such a definition of  $h_T$  have no significance outside of the experimental context, but it also is an unrealistic model for the kinetics of transitions<sup>9</sup>.

## REFERENCES

- 1 M. J. O'Neill, *Anal. Chem.*, 38 (1966) 1331.
- 2 C. M. Guttman and J. H. Flynn, *Anal. Chem.*, 45 (1973) 408.
- 3 A. P. Gray and R. L. Fyans, Pittsburgh Conference on Analytical Chemistry, March (1973).
- 4 D. A. Ditmars and T. B. Douglas, *J. Res. Nat. Bur. Stand.*, 75A (1971) 401.
- 5 C. M. Guttman, personal communication, 1973.
- 6 J. H. Flynn, in H. G. Wiedemann (editor), *Thermal Analysis (3 ICTA)*, Vol. 1, Birkhauser Verlag, Basel and Stuttgart, 1972, pp. 127-138.
- 7 S. S. Chang, *J. Polym. Sci. C, 2nd Int. Symp. Polym. Characterization*, in press.
- 8 R. C. Mackenzie et al., *Talanta*, 19 (1972) 1079.
- 9 W. P. Brennan, B. Miller and J. C. Whitwell, *Ind. Eng. Chem. Fundam.*, 8 (1969) 314.